Tailored Acoustic Holograms with Phased Arrays

Iablonskyi, Denys

IEEE
2022

Iablonskyi , D , Sundblad , F A , Wuensch , B , Klami , A , Salmi , A & Haeggström , E 2022 , Tailored Acoustic Holograms with Phased Arrays . in 2022 IEEE International Ultrasonics Symposium (IUS) . IEEE , 2022 IEEE International Ultrasonics Symposium (IUS) , Venice , Italy , 10/10/2022 . https://doi.org/10.1109/IUS54386.2022.9957750

http://hdl.handle.net/10138/354155
https://doi.org/10.1109/IUS54386.2022.9957750

submittedVersion

Tailored Acoustic Holograms with Phased Arrays

Denys Iablonskyi
Departments of Computer Science and Physics, University of Helsinki
Helsinki, Finland
denys.iablonskyi@helsinki.fi

Felix Sundblad
Department of Physics
University of Helsinki
Helsinki, Finland
felix.sundblad@helsinki.fi

Bruno Wuensch
Department of Physics
University of Helsinki
Helsinki, Finland
bruno.wuensch@epfl.ch

Arto Klami
Departments of Computer Science
University of Helsinki
Helsinki, Finland
arto.klami@helsinki.fi

Ari Salmi
Physics Department,
University of Helsinki
Helsinki, Finland
ari.salmi@helsinki.fi

Edward Hæggström
Department of Physics
University of Helsinki
Helsinki, Finland
edward.haeggstrom@helsinki.fi

***Abstract*— Advances in phased array of transducers (PATs) allow for precise control of each element's phase and amplitude and can consist of hundreds of transducers. The widely adopted Gerchberg–Saxton type of algorithms do not provide sufficient accuracy for complex control tasks like formation of detailed holograms as they perform well only for a small number of control points with respect to the number of transducers. Here we present an efficient PATs amplitude and phase solver based on the iterative first-order gradient optimization of the user defined loss function (APGO). We demonstrate high resolution hologram reconstruction when the number of control points is 25 times the number of transducers.**

Keywords—acoustic holography, levitation, phased array, ultrasound

I. Introduction

In recent years, acoustic holography has gained significant attention and several experimental and computational techniques has been developed [1-6]. A typical method for manipulating acoustic wavefront is to use phased array of transducers (PATs), which is a set of ultrasonic transducers that can be arranged in different geometries with controllable phases and amplitudes. The applications range from manipulation of acoustically levitated objects [1, 2, 6] to volumetric and tactile displays [3, 5]. The PATs driving parameters can be readjusted during the operation which allows for dynamic control of the generated acoustic field. The main task is to find the transducers activation function i.e., to solve the inverse problem from desired acoustic field or radiation forces to PATs phases and amplitudes.

It has been shown that already direct gradient-based optimization of the PATs phases outperforms the conventional Gerchberg–Saxton algorithms in the tasks of reconstructing target pressure fields [4]. In this paper we present the amplitude and phase gradient optimizer (APGO) for user defined PATs geometry and objective function. We show that optimization of amplitudes in addition to phases further increases the hologram reconstruction quality. Moreover, the high performance of the algorithm allows for real-time optimization of the video sequence when the neighboring frames change smoothly.

II. Method

Time-averaged acoustic sound field created by PATs at the point in space $\boldsymbol{r}_n$ within a linear regime is a superposition of the sound waves emitted by each individual transducer:

$$P_n(\boldsymbol{\alpha}, \boldsymbol{\varphi}, \boldsymbol{r}_n) = \sum_m p(\alpha_m, \varphi_m) e^{ikr_{mn}}, \qquad (1)$$

where $p(\alpha_m, \varphi_m)$ is the m-th transducer's activation function characterized by the amplitude α_m and the phase φ_m, k is the wavenumber, and r_{mn} is the distance from the m -th transducer to the point $\boldsymbol{r}_n$. The acoustic pressure field (1) generated by M transducers at the set of points N can be written in matrix form $\boldsymbol{P} = \boldsymbol{pT}$, where $\boldsymbol{T}$ is the transmission matrix of $[M \times N]$ size that accounts for phase transfer and transducer directivity function from each transducer m to each point n. For a fixed PATs geometry and fixed target image coordinates the transmission matrix is constant and needs to be calculated only once at the beginning of the optimization procedure. Thus, the total pressure field in the region of interest can be efficiently calculated by single matrix multiplication.

To create a desired acoustic pressure image A_n that consists of low- and high-pressure pixels at locations $\boldsymbol{r}_n$ we formulate an optimization problem that minimizes the discrepancy between the target pressure A_n and PATs absolute pressure field $|P_n|$ for each pixel in the space. The quality of the generated pressure filed can be expressed as a mean squared error (MSE):

$$\mathcal{L}(\boldsymbol{\alpha}, \boldsymbol{\varphi}) = \sum_n (A_n - |P_n(\boldsymbol{\alpha}, \boldsymbol{\varphi}, \boldsymbol{r}_n)|)^2 . \qquad (2)$$

The optimization problem thus is to find arguments $\{\alpha_m\} \in [0, p_0]$ and $\{\varphi_m\} \in [0, 2\pi]$ that minimize the objective function (2):

$$\underset{\boldsymbol{\alpha}, \boldsymbol{\varphi}}{\arg\min}\, \mathcal{L}(\boldsymbol{\alpha}, \boldsymbol{\varphi}). \qquad (3)$$

The optimization procedure was implemented in *Python* programing language using open-source machine learning framework *PyTorch* [7]. We use the *Adam* optimizer for solving the minimization problem (3), using automatic differentiation for computing the derivatives with respect to amplitudes and phases. *Adam* is an adaptive first-order gradient-based stochastic algorithm. We found it to be more robust comparing to stochastic gradient descent *SGD* while offering similar accuracy as a second-order quasi-Newton *LBFGS* algorithm but at a fraction of the computational cost.

The form of the loss function can be freely chosen e.g., to increase the contrast of the generated pressure filed or to reduce the noise as we will see in Sec. III. Due to the use of automatic differentiation for computing the derivatives, we can use any differentiable loss, and empirical testing of alternatives is efficient as the optimizer does not need to be changed. Note that (2) accounts only for the absolute pressure field without limiting the phase profile, this naturally allows for higher quality hologram reconstruction by modulating non-interfering phase image. To increase pressure output for

This work was supported by the Academy of Finland (project codes 324852, 336019, and 336020).

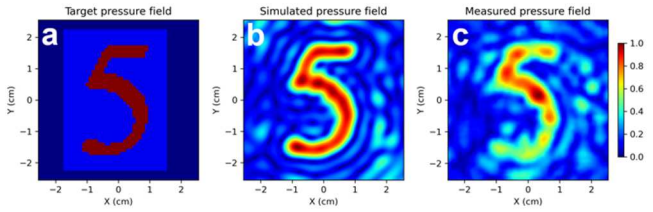

Fig. 1. Hologram reconstruction using APGO algorithm for 2 hemispherical PATs. a) Target pressure image of 50×50 pixels in XY-plane, the highlighted area shows the optimization mask. b) Simulated pressure field using APGO. c) Measured pressure field using waveguide.

practical application one can include an additional term $\sum_m |p_m|$ in (2) which requires to optimize target pressure field with the lowest power consumption of PATs.

The optimization problem described above solves the PATs configuration for holograms, but the same principle can be used also for acoustic levitation. This only requires changing the objective into one that considers radiation forces acting on the object:

$$\mathcal{L}(\boldsymbol{\alpha}, \boldsymbol{\varphi}) = c_1 |\boldsymbol{F}(\boldsymbol{r}) + \boldsymbol{G}| + c_2 \nabla \boldsymbol{F} + c_3 |\nabla \times \boldsymbol{F}|, \qquad (4)$$

where c_i are the normalizing weights, $\boldsymbol{F}(\boldsymbol{r})$ is the net radiation force, and $\boldsymbol{G}$ is the gravitational force. The first term in (4) requires net zero force, the second term describes restoring force towards the center of the trap and the third one reduces the curl of the force field.

III. Results & Discussion

A. Experimental validation

We first start with experimental validation of the proposed optimization algorithm. Our previously designed PATs [8] consists of 450 ultrasonic transducers (40 kHz central frequency, 1 cm in diameter) arranged into 2 hemispheres of 15 cm diameter facing each other. The phase, amplitude and frequency can be set independently for each transducer via 4 FPGAs. The phase offsets of each transducer were calibrated at the geometrical center of the PATs. The total pressure fields in the XY-plane were measured by moving the waveguide mounted on a two-axis translation stage.

Fig. 1 depicts the experimentally measured pressure field in the XY-plane that was generated with 2 hemispherical PATs. The target field is an image of 50×50 pixels of $\{0, 1\}$ intensity. The pixel size was 1 mm ($\lambda = 8.6$ mm). The activation function was then obtained by APGO via minimization of the MSE between the target and the generated pressure field within the region of interest (Fig. 1a). The reconstructed image resembles well the target image, while the measured field shows some discrepancies in the intensity. This is caused by the fact that the PATs phases were calibrated at the center and the phase shift at any other location is calculated based on the geometrical consideration of the transducers whose locations are known only approximately. In addition, transducers do not always have the same maximum output and taking it into account during the optimization stage can further improve the experimental accuracy.

B. Optimization procedure

We consider a single-sided flat configuration PATs of 20×20 transducers placed 10 cm from the image plane. The target pressure image is 100×100 pixels with the pixel size

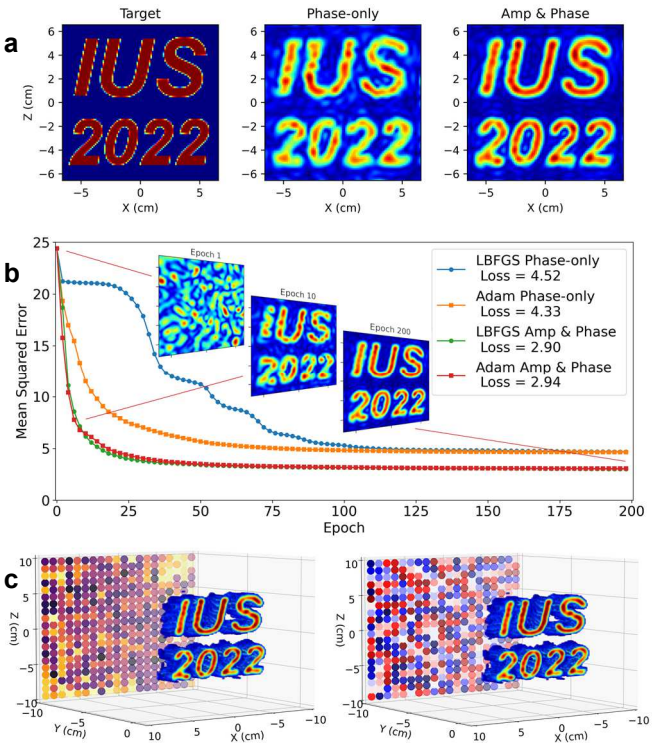

Fig. 2. Simulation results. Hologram reconstruction for 100×100 target image using flat configuration PATs of 20×20 transducers. a) Reconstruction comparison between phase-only optimization and phase and amplitude optimization. b) Convergence of the loss function for *Adam* and *LBFGS* optimizers. c) 3D plot of the pressure distribution and transducers amplitudes (left) and phases (right), for visual purpose the pressures are shown between 0.2 and 1.

1.2 mm (Fig. 2). The optimization procedure starts with randomized transducers phases and equal amplitudes (Fig. 2b). After propagating the activation function to all target pixels and calculating resulting acoustic pressure the algorithm automatically estimates the gradients of the loss function and adjusts the parameters accordingly. We compare two optimization algorithms, first-order adaptive gradient optimization *Adam* and second-order quasi-Newton method *LBFGS*. Optimization of the single valued loss function that depends on hundreds or thousands of parameters is a non-convex task. Allowing for amplitude optimization in addition to phase optimization can help finding a globally optimal solution. Fig. 2 (a, b) reveal that simultaneous optimization for amplitudes and phases improves the hologram reconstruction accuracy reducing MSE by 32%. Even though the *LBFGS* algorithm accounts for gradient curvature, we saw no improvements over the more robust and faster *Adam* algorithm.

C. Objective fuction

As described in Sec. II the objective function summarizes the problem formulation and in case of PATs it can describe the levitation task or the hologram reconstruction. Here we show how defining the loss function can affect the image reconstruction. Commonly used in gradient optimizations mean squared error (MSE) emphasizes larger discrepancies between the target and the reconstructed images. Instead, the mean absolute error (MAE) weights all discrepancies equally. Thus, minimizing the MAE loss function results in lower background reconstruction noise, while MSE better

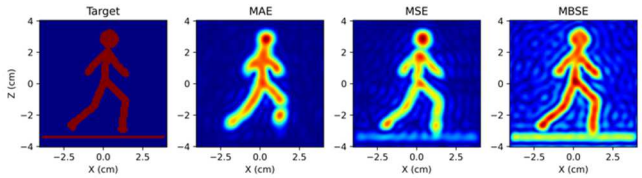

Fig. 3. Comparison of hologram reconstruction using different error measures.

recovers target image shape (Fig. 3). To emphasize the high intensity pixels in the reconstruction image we can further increase the contrast, at the expense of higher background noise, using the mean bi-squared error (MBSE) i.e., $\sum(A^2 - |P|^2)^2$.

The simulations were performed using single-sided flat configuration PATs of 20×20 transducers at 10 cm distance from the image plane. The target pressure image is 100×100 pixels with a pixel size of 0.8 mm.

D. Computational performance

In the above optimizations of 10000 control points with 400 transducers the average computational time was 8 s for 100 iterations on an average laptop computer (1.6 GHz Core i5-8210Y, 16 GB RAM) to achieve reasonable reconstruction accuracy. Several other computational times are presented in Table I for 100 iterations. We see that for holograms of slightly lower resolution (fewer control points), it is feasible to solve for the configuration at speeds sufficient for real-time displays, especially if considering PATs of slightly fewer transducers of faster hardware. The APGO algorithm is thus suitable for generation of the holographic movies when the video sequence is changing smoothly. Once the convergence is achieved, the subsequent re-optimization for the next frames takes substantially less iterations.

IV. Conclusions

We presented the PATs amplitude and phase gradient optimizer APGO and showed that the amplitude optimization, in addition to the phase, further improves the hologram reconstruction accuracy. The reconstruction of holograms consisting of thousands of points can be performed in a matter of seconds and smaller ones in fractions of second, sufficient even for real-time optimization of the smooth video sequence. The exact characteristics of the hologram can easily be controlled by manipulating the error metric. The flexibility with respect to hologram error metric allows to address different tasks such as acoustic levitation. The APGO algorithm is expected to be useful especially in more challenging levitation tasks e.g., levitation of bigger objects and their dynamic manipulation.

TABLE I.
Computational time for 100 iterations with 400 transducers

Control points	100	900	2500	10000
Computational time (s)	0.2	0.76	2.5	8

References

[1] K. Melde, A. Mark, T. Qiu et al., “Holograms for acoustics”, Nature 537, 518–522 (2016).

[2] A. Marzo, S. Seah, B. Drinkwater et al., “Holographic acoustic elements for manipulation of levitated objects”, Nat Commun 6, 8661 (2015).

[3] R. Hirayama, D. M. Plasencia, N. Masuda et al., “A volumetric display for visual, tactile and audio presentation using acoustic trapping”, Nature 575, 320–323 (2019).

[4] T. Fushimi, K. Yamamoto, and Y. Ochiai, “Acoustic hologram optimisation using automatic differentiation”, Sci Rep 11, 12678 (2021).

[5] R. Hirayama, G. Christopoulos, D. M. Plasencia, and S. Subramanian, "High-speed acoustic holography with arbitrary scattering objects", Science Advances 8, 24 (2022).

[6] S. Inoue, S. Mogami, T. Ichiyama, A. Noda, Y. Makino, and H. Shinoda, “Acoustical boundary hologram for macroscopic rigid-body levitation”, J. Acoust. Soc. Am. 145(1), 328–337 (2019).

[7] A. Paszke et al., ”PyTorch: An Imperative Style, High-Performance Deep Learning Library”, In Advances in Neural Information Processing Systems 32. Curran Associates, Inc., pp. 8024–8035 (2019).

[8] T. Puranen, P. Helander, A. Meriläinen, G. Maconi, A. Penttilä, M. Gritsevich, I. Kassamakov, A. Salmi, K. Muinonen, and E. Haeggström, “Multifrequency acoustic levitation”, in IEEE International Ultrasonics Symposium, pp. 916–919 (2019).